Journal of Alloys and Compounds 509 (2011) 152–156

Contents lists available at ScienceDirect

Journal of Alloys and Compounds

journal homepage: www.elsevier.com/locate/jallcom

Kinetics of 9-ethylcarbazole hydrogenation over Raney-Ni catalyst for hydrogen storage

Xufeng Ye, Yue An*, Guohua Xu

Department of Chemical and Biological Engineering, Zhejiang University, Hangzhou 310027, PR China

ARTICLE INFO

Article history:
Received 13 July 2010
Received in revised form 1 September 2010
Accepted 1 September 2010
Available online 15 September 2010

Keywords:
9-Ethylcarbazole
Catalytic hydrogenation
Raney-Ni catalyst
Kinetics
Hydrogen storage

ABSTRACT

Hydrogen storage in form of liquid organic hydrides, e.g. 9-ethylcarbazole, is a relatively novel method. In the present work, the hydrogenation kinetics of 9-ethylcarbazole over Raney-Ni catalyst was studied by investigating the influences of the reaction temperature, pressure and catalyst concentration on the mass transfer-reaction processes. The results show that the kinetics of reaction is controlled by the chemical process on the catalyst surfaces. The hydrogenation reaction followed first-order kinetics with an apparent activation energy of 65.17 KJ/mol. The apparent kinetics model of the hydrogenation was established.

1. Introduction

Hydrogen has often been suggested as a potential energy carrier in automotive applications. It is thought to be one of the most promising clean energy without emissions of greenhouse gases, which can be renewable, efficient and produced from a variety of sources including fossil fuels, and even water (by means of nuclear, wind or solar energy). However, there are still many problems to implement hydrogen economy in daily life, out of which hydrogen storage is major bottleneck. Due to these reasons tremendous efforts have been made to search hydrogen storage materials which can hold hydrogen reversibly with high energy density [1,2]. As a target given by the U.S. Department of Energy (DOE), the storage criteria for vehicular applications are 5.5 wt.% storage capacity and H_2 release at temperatures below 473 K in low cost and low toxicity [3]. According to a study funded by DOE, for traditional PEM fuel cell, it would require 3.58 kg payload of hydrogen when driving 480 km. At present, the working temperatures of the novel high temperature PEM fuel cells can be as high as 393–453 K. By translating vehicle performance requirements into storage system needs, the energy density of hydrogen should approach the storage criteria described by DOE to achieve a comparable driving range [4].

Hydrogen gas has a low density, low temperature of its liquefaction, as well as high explosive risk in combination with its negative influence on the properties of design materials. In addition, metal containers easily form hydrides with hydrogen, making it become brittle. Therefore, it is an important research to explore effective and safe hydrogen storage methods [5].

Hydrogen storage in form of liquid organic hydrides (namely storing hydrogen covalently as part of a molecule) is a relatively novel method. Compared to other hydrogen storage approaches including compressed hydrogen gas, cryogenic and liquid hydrogen, metal hydrides and high surface area sorbents, the advantages of hydrogen storage in form of liquid organic hydrides are high energy density, safe transportation, etc [6]. Table 1 shows the list of some liquid hydrogen storage materials and reports the gravimetric hydrogen storage value.

In spite of its many advantages the attractive possibility of using an organic liquid as storage medium has not yet received sufficient attention in the past, even widely excluded from consideration because low temperature H_2 release has not been thought feasible (reaction temperatures require 600–700 K) [7–9]. Recently, Alan Cooper and Guido Pez at Air Products [10] first reported using the aromatic molecules with heteroatom(s) for new hydrogen storage media in a series of patents [11,12]. 9-Ethylcarbazole is an example of these heterocyclic compounds. In their research, it was shown that incorporation of N in the 9-ethylcarbazole can decrease the endothermicity of the reaction and bring down dehydrogenation temperature. Thus, the possibility of hydrogen storage and release can be realized according to reaction equation of 9-ethylcarbazol hydrogenation at Table 1.

Nowadays the available literature data concerning hydrogen storage properties of 9-ethylcarbazole are very limited. Furthermore, there is no in-depth study about the hydrogenation

* Corresponding author. Tel.: +86 571 87951742; fax: +86 571 87951742.
E-mail addresses: anyue@zju.edu.cn, zju.anyue@gmail.com (Y. An).

0925-8388/$ – see front matter © 2010 Elsevier B.V. All rights reserved.
doi:10.1016/j.jallcom.2010.09.012

Table 1
Hydrogen storage properties of some hydrogen storage materials.

Hydrogen storage system	Reaction equation	The theoretical gravimetric storage capacity (%)
Benzene	$C_6H_6 + 3H_2 \Leftrightarrow C_6H_{12}$	7.19
Toluene	$C_7H_8 + 3H_2 \Leftrightarrow C_7H_{14}$	6.16
Naphthalene	$C_{10}H_8 + 5H_2 \Leftrightarrow C_{10}H_{18}$	7.29
9-Ethylcarbazole	$C_{14}H_{13}N + 6H_2 \Leftrightarrow C_{14}H_{25}N$	5.8

kinetics of 9-ethylcarbazole. In present work, the kinetics of 9-ethylcarbazole have been studied over Raney-Ni catalyst. The influences of the temperature, system pressure, catalyst concentration on the hydrogenation reaction rates of 9-ethylcarbazole were investigated. Moreover, the apparent kinetics model of the hydrogenation reaction was established.

2. Experimental

2.1. Materials

The reactions were conducted in a 0.3L FYX-D03 stainless steel autoclave with magnetic stirring, as seen in Fig. 1. The hydrogen reservoir has a certain capacity, the reactor was filled with ultra high purity hydrogen (99.99% pure) from the hydrogen reservoir. Thus, the hydrogen absorption capacity was calculated by measuring the hydrogen pressure decrease in the hydrogen reservoir.

The activated Raney-Ni catalyst was purchased from Zhejiang Metallurgical Research Institute. The apparent density and the mean particle size of Raney-Ni catalyst are 3.0 g/cm^3 and 16.58 μm, respectively. 9-Ethylcarbazole (99.5%) was purchased from ShangHai Infine chemical company.

2.2. Catalytic hydrogenation of 9-ethylcarbazole

Ten grams of 9-ethylcarbazole followed by the activated Raney-Ni catalyst were putted in the stainless steel autoclave with continuous monitoring of stirrer speed, temperature and pressure. The reactor was then sealed, evacuated for about 15 min, flushed with hydrogen and then heated to the desired temperature. Afterwards, the reaction was started at the desired temperature and pressure while stirring at a speed of 1000 rpm. As the reaction proceeds, the pressure in the reactor was held constant over the entire experiment by adding the hydrogen continuously from the reservoir. The quantity of the consumed hydrogen was recorded by the pressure gauge and the reaction time was measured. The liquid reaction products were analysed using a gas chromatograph–mass spectrometer (HP6890/5973GC-MS).

3. Results and discussion

3.1. Influence of temperature on the hydrogenation of 9-ethylcarbazole

From Fig. 2, which showed the hydrogen absorption curves of 9-ethylcarbazole at 120 °C, 140 °C, 160 °C, 180 °C, 200 °C, 220 °C and 240 °C with 1.0 g Raney-Ni catalyst and 5.0 MPa reaction pressure, it can be seen that the reaction rate accelerates with increased temperature from 120 °C to 200 °C, which reaches the maximum

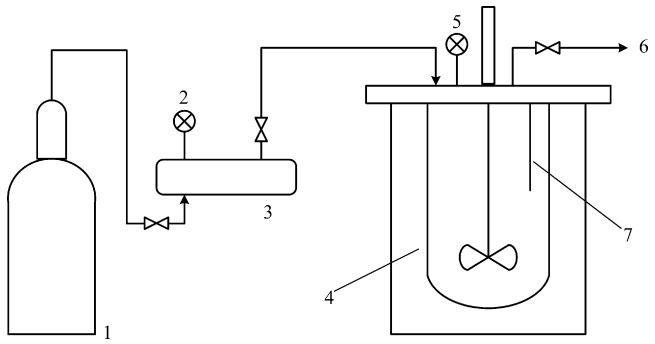

Fig. 1. Schematic diagram of the experimental system. 1, hydrogen source; 2, 5, pressure gauge; 3, hydrogen reservoir; 4, stainless steel autoclave; 6, vent pipe; 7, thermocouple.

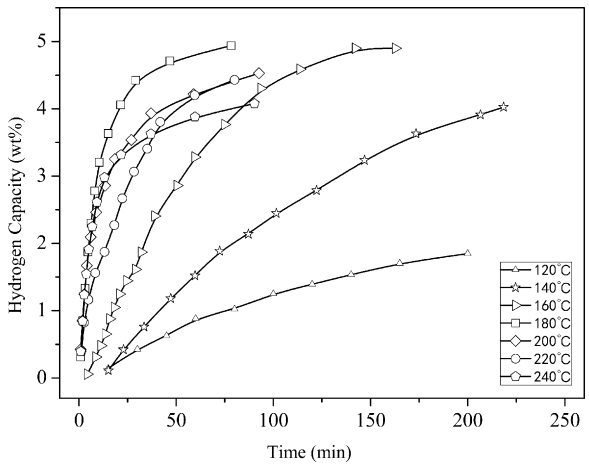

Fig. 2. Hydrogen absorption in 9-ethylcarbazole measurements at 240 °C, 220 °C, 200 °C, 180 °C, 160 °C, 140 °C and 120 °C at 50 bar H_2 over 10 wt.% Raney-Ni.

reaction rate at about 200 °C, whereas the hydrogen uptake of 9-ethylcarbazole reaches the maximum value (5.0 wt.%) at 180 °C. However, when the temperature further increases to 240 °C, the hydrogen uptake decreased to 4.08 wt.%. The decrease in reaction rate may be caused by the drop of the catalyst activity at high temperature. On the other hand, the mass transfer of hydrogen might be limited at high temperature in this system, as also reported in Ref. [13]

3.2. Influence of reaction pressure on the hydrogenation of 9-ethylcarbazole

The hydrogen absorption curves (Fig. 3) were measured under various pressures at 200 °C to investigate the effect of the reaction pressure on the reaction rate. It was exhibited that with the rise in the reaction pressure, the reaction rate increases, as well as the hydrogen absorption capacity. When the hydrogen pressure is 2.0, 3.0, 4.0, 5.0, and 6.0 MPa, the hydrogen uptake reaches 3.55 wt.%, 4.21 wt.%, 4.36 wt.%, 4.92 wt.%, and 5.0 wt.%, respectively. Hydrogenation of 9-ethylcarbazole is the reaction of volume reduced, therefore increment of the reaction pressure is beneficial for the hydrogenation reaction, with the improvement of the hydrogen solubility, which leads to higher reaction rate and the shifting of reaction equilibrium to product direction, and also with the

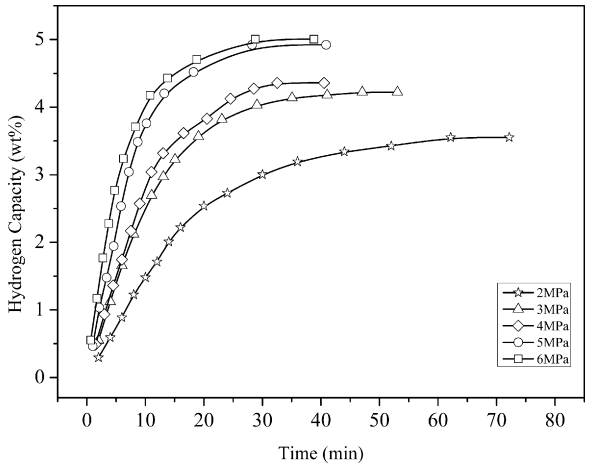

Fig. 3. Hydrogen absorption in 9-ethylcarbazole measurements at 2.0 MPa, 3.0 MPa, 4.0 MPa, 5.0 MPa and 6.0 MPa H_2 at 200 °C over 10 wt.% Raney-Ni.

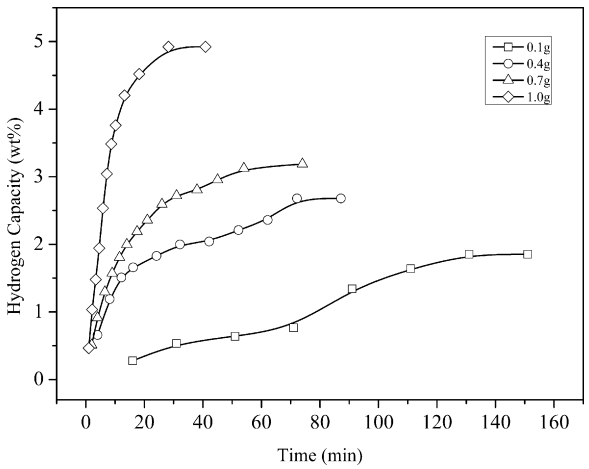

Fig. 4. Hydrogen absorption in 9-ethylcarbazole measurements at 200 °C and at 5.0 MPa H_2 over 1 wt.%, 4 wt.%, 7 wt.%, and 10 wt.% Raney-Ni.

restraint of the carbon deposition on the catalyst, which extends the life of the catalyst.

3.3. Influence of catalyst concentration on the hydrogenation of 9-ethylcarbazole

The hydrogenation of 9-ethylcarbazole was carried out using a range of Raney-Ni catalyst dosage from 1 wt.% to 10 wt.% at 200 °C to determine the effect of catalyst concentration on reaction rate (Fig. 4). The hydrogen absorption curves over time at 200 °C and 5.0 MPa, as shown in Fig. 4, suggested that the concentration of catalyst could influence the reaction rate in certain content. Accordingly, with the increasing of the Raney-Ni catalyst dosage, the reaction rate gradually increased and the hydrogen absorption capacity was raised from 1.85 wt.% to 4.92 wt.%.

3.4. Kinetic analysis of 9-ethylcarbazole hydrogenation reaction

3.4.1. Mass transfer process of the hydrogenation reaction

The hydrogenation process of 9-ethylcarbazole over Raney-Ni catalyst is a gas–liquid–solid tri-phases mass transfer process, as shown in Fig. 5. The hydrogen gas transfers from bulk gas through the gas film to the gas–liquid interface, where it is absorbed by the surrounding liquid, then the absorbed hydrogen diffuses from the bulk liquid to the surface of the solid catalyst, where the catalytic hydrogenation takes place. Due to the use of pure hydrogen as reactant, the mass transfer resistance occurred in the gas film side of the gas–liquid interface can be ignored.

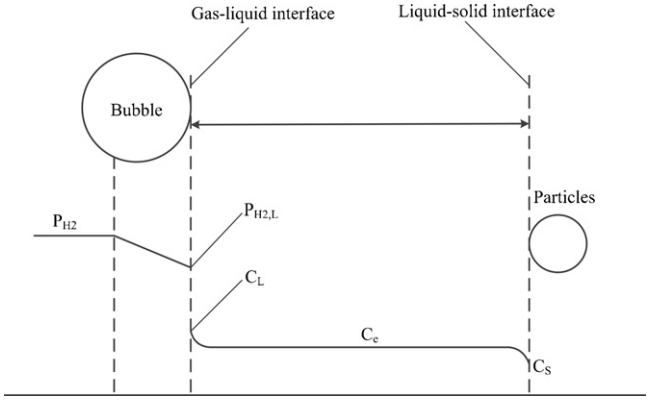

Fig. 5. Schematic diagram of concentration distribution in the gas–liquid–solid reaction process.

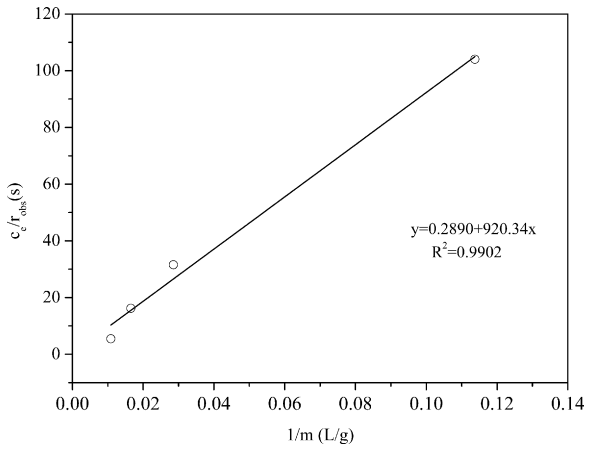

Fig. 6. Relationship between c_e/robs and $1/m$ (T: 473 K, p: 5.0 MPa, N: 1000 rpm, 10 g $C_{14}H_{13}N$ in the slurry).

In combination with our previously studies on mass-transfer and reaction process in similar system [14,15], the apparent reaction rate equation of 9-ethylcarbazole hydrogenation can be written as:

$$\frac{c_e}{r_{obs}} = \frac{1}{k_L a_g} + \frac{\rho_p d_p}{6m}\left(\frac{1}{k_c} + \frac{1}{k_s}\right) \quad (1)$$

in which r_{obs} is the apparent reaction rate, c_e is the concentration of the hydrogen in the liquid phase, k_c is the liquid–solid mass transfer coefficient, k_L is the gas–liquid mass transfer coefficient on the liquid side at the gas–liquid interface, k_s is the reaction rate constant at the solid surface (m/s), a_g is the specific surface area of bubbles per unit liquid volume, m is the catalyst load per unit liquid volume, ρ_p is the density of the solid particle and d_p is the mean particle size. The Eq. (1) shows that in hydrogenation process of 9-ethylcarbazole the total resistance (c_e/r_{obs}) mainly includes: the mass transfer resistance on the liquid side at gas–liquid interface ($1/k_L a_g$), the mass transfer resistance of hydrogen from bulk liquid to the surface of the catalyst particles ($(\rho_p d_p/6m)(1/k_c)$), the reaction resistance at the surface of the catalyst particles ($(\rho_p d_p/6m)(1/k_s)$).

For the 9-ethylcarbazole hydrogenation reaction in present study, according to Eq. (1), the mass transfer resistance on the liquid side at gas–liquid interface ($1/k_L a_g$) is determined by linear regression according to the c_e/r_{obs} vs $1/m$ plot. Moreover, the mass transfer resistance at the liquid–solid interface ($\rho_p d_p/6m$) ($1/k_c$) is obtained based on the calculation of k_c. Because of the existence of strong stirring during the hydrogenation reaction process, it is actually a mass transfer between flowing liquid and moving particles [16]. Thus, liquid–solid mass transfer coefficient k_c can be calculated from Sherwood Number, using the following equation:

$$\mathrm{Sh} = \frac{k_c^* d_p}{D} \quad (2)$$

With a view to the effect of fluid turbulence caused by the intensely stirring, the mass transfer coefficient k_c is usually revised by double the calculated value k_c^* [17,18]. Subsequently, the total resistance is compared with the sum of the liquid–solid mass transfer resistance ($(\rho_p d_p/6m)(1/k_c)$) together with the gas–liquid mass transfer resistance ($1/k_L a_g$) in order to obtain the reaction resistance at the surface of the catalyst particles ($(\rho_p d_p/6m)(1/k_s)$).

3.4.2. Parameters calculation of kinetic model

According to Eq. (1) together with the experimental data obtained at various catalyst concentrations (Fig. 4), c_e/r_{obs} was plotted versus $1/m$ in Fig. 6, which showed a good linear relationship correlations between the two terms, with the slop $(\rho_p d_p/6)((1/k_c)+(1/k_s))$ being 920.34 s g L^{-1}, and the intercept

Table 2
Comparison of the mass transfer resistance ($1/k_c$) and reaction resistance ($1/k_s$).

T (K)	$D^a \times 10^5$ (cm^2/s)	Pe[b]	Sh[c]	$k_c{}^{*d} \times 10^4$ (m/s)	$1/k_c$ (s/m)	c_e (mol/L)	r_{obs} (mol/m^3 s)	c_e/r_{obs} (s)	$1/k_s{}^e \times 10^{-6}$ (s/m)	$k_s \times 10^7$ (m/s)
393	2.981	0.629	2.211	3.98	1258	0.0735	0.7575	97.07	1.1277	8.868
413	4.554	0.602	2.205	6.06	825.4	0.0792	1.938	40.84	0.4691	21.32
433	6.404	0.577	2.199	8.50	588.5	0.0849	5.4949	15.46	0.1753	57.06
453	8.694	0.554	2.195	11.5	434.4	0.0909	15.684	5.79	0.06472	154.5
473	11.267	0.533	2.189	14.9	335.9	0.0971	23.507	4.13	0.04549	219.8

[a] Diffusivity of hydrogen in 9-ethylcarbazole $D_{1,2}^{[18]} = 7.4 \times 10^{-15} \frac{(\psi \cdot M)^{1/2} T}{\mu \tilde{V}_1^{0.6}}$, $\tilde{V} = 14.3\,\text{cm}^3/\text{mol}$.

[b] $\text{Pe}^{[17]} = \frac{g \cdot d_p^2 \cdot \Delta\rho}{18\mu D}$.

[c] $\text{Sh}^{2[16,17]} = 4.0 + 1.21\text{Pe}^{2/3} (0 < \text{Pe} < 1000)$.

[d] $k_c^{*[17]} = \frac{\text{Sh} \cdot d_p}{D}$; usually, $k_c = 2k_c^*$, according to Ref. [17], Chap.8.

[e] Calculated using Eq. (1).

$1/k_L a_g$ being 0.2890 s. Through comparison, it was found that in the hydrogenation process of 9-ethylcarbazole under the catalyst concentration of 1–10 wt.%, the value of $1/k_L a_g$ was significantly smaller than $(\rho_p d_p/6)((1/k_c)+(1/k_s))$. As a result, the mass transfer resistance on the liquid side at gas–liquid interface ($1/k_L a_g$) in Eq. (1) could be negligible.

Based on the obtained rate of 9-ethylcarbazole hydrogenation at each temperature (Fig. 2), the apparent reaction rate constant k_s, as well as the liquid–solid mass transfer coefficient k_c were derived. The data used in the calculation are summarized in Table 2 together with the calculated result. The comparison between $1/k_c$ and $1/k_s$ in Table 2 shows that $1/k_c$ which is significantly smaller can be neglected, with the whole process controlled completely by surfaces reaction. Subsequently, kinetic model described by Eq. (1) can be simplified as follows:

$$r_{obs} = k_s \cdot \frac{6m}{\rho_p d_p} \cdot c_e \tag{3}$$

in which k_s, the apparent reaction rate constant, follows the Arrhenius equation:

$$k_s = k_{s,0} \cdot e^{-\Delta Ea/RT} \tag{4}$$

Using the obtained rate constants k_s at each temperature in Table 2, the logarithm of the kinetic rate constants was plotted versus the reciprocal temperature, as shown in Fig. 7. The frequency factor $k_{s,0}$ and the apparent activation energy ΔEa were estimated to be 4.06×10^2 m/s and 65.17 KJ/mol, respectively. For 9-ethylcarbazole hydrogenation at a range of reaction temperature from 120 °C to 200 °C on 10 wt.% catalyst concentration, the

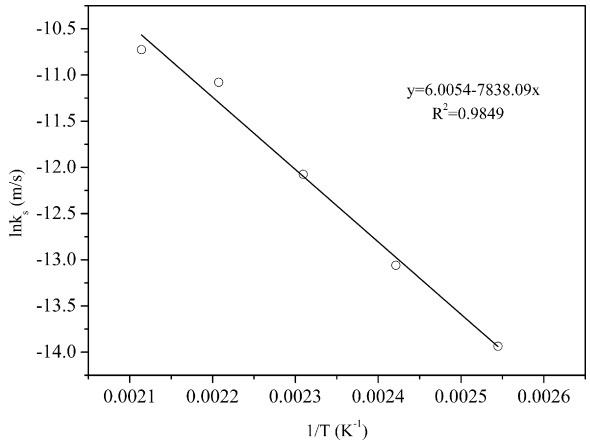

Fig. 7. Relationship between $\ln k_s$ and $1/T$ (p: 5.0 MPa, N: 1000 rpm, slurry composition: 10 g $C_{14}H_{13}N$ + 1 g Raney-Ni).

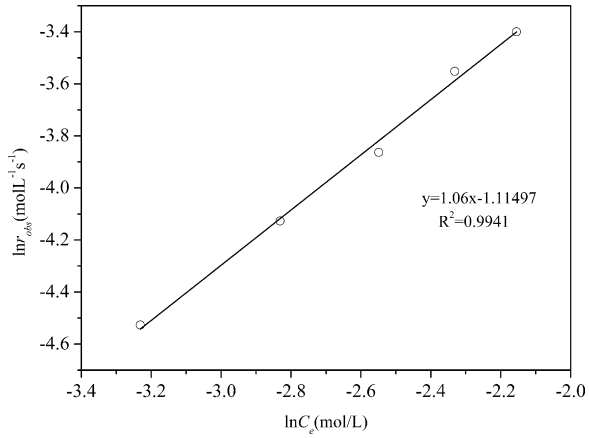

Fig. 8. Relationship between $\ln r_{obs}$ and $\ln c_e$ (T: 473 K, N: 1000 rpm, slurry composition: 10 g $C_{14}H_{13}N$ + 1 g Raney-Ni).

apparent kinetics model can be written as:

$$r_{obs} = 4.06 \times 10^2 \cdot e^{-6.517 \times 10^4/RT} \cdot \frac{6m}{\rho_p d_p} \cdot c_e \tag{5}$$

In order to test and verify the above kinetic model using the experimental data obtained at various hydrogen pressures and a temperature of 200 °C shown in Fig. 2, it was assumed that the reaction was nth order in the liquid-phase hydrogen concentration as follows:

$$r_{obs} = k_s a_p \cdot {c_e}^n \tag{6}$$

Subsequently, $\ln r_{obs}$ was plotted versus $\ln c_e$ to obtain the linear regression profile shown in Fig. 8, which gave:

$$r_{obs} = 0.3279 \cdot {c_e}^{1.06} \tag{7}$$

On the other hand, $k_s a_p$ can also be determined by the obtained apparent kinetic model. According to Eq. (5), the value of $k_s a_p$ at the temperature of 200 °C was estimated to be 0.299 s^{-1}, which was in agreement with the value in Eq. (7). Considering the experimental errors in actual measurement ands and the simplification in calculation, it is reasonable to envisage that the reaction is first order in the liquid-phase hydrogen concentration and the model gave the best fit of experimental data.

4. Conclusions

(1) 9-Ethylcarbazole hydrogenation over Raney-Ni catalyst was studied in the temperature range 120–240 °C and the pressure range 2.0–6.0 MPa. The whole reaction process is controlled by the surface reaction of the catalyst particles. The mass transfer resistance at gas–liquid interface and that from the bulk liquid phase to the surface of the catalyst particles can be ignored.

(2) Raney-Ni catalyst exhibited strong performance to the hydrogenation of 9-ethylcarbazole. The reaction rate accelerated with increased temperature, and the initial reaction rate reached the maximum at about 200 °C, whereas the hydrogen uptake of 9-ethylcarbazole reaches the maximum value (5.0 wt.%) at 180 °C. However, when the temperature exceeded 200 °C, the reaction rate went down.

(3) The apparent reaction rate was zero order for the concentration of 9-ethylcarbazole and first order for hydrogen concentration in the liquid phase. In the temperature range of 120–200 °C, the apparent kinetics model can be written as:

$$r_{obs} = 4.06 \times 10^2 \cdot e^{-6.517\times10^4/RT} \cdot \frac{6m}{\rho_p d_p} \cdot c_e$$

Acknowledgements

This work is supported by the National High Technology Research & Development Program of China (2007AA05Z112) and National Basic Research Program of China (2007CB209700).

References

[1] B. Bogdanovic, M. Schwickardi, J. Alloys Compd. 253–254 (1997) 1–9.
[2] I.P. Jain, P. Jain, A. Jain, J. Alloys Compd. 503 (2010) 303–339.
[3] S. Satyapal, FY2006 DOE Hydrogen Program Annual Merit Review and Peer Evaluation Meeting Proceedings, Plenary Session. Available at: http://www.hydrogen.energy.gov/annual-review06-plenary.html, 2006.
[4] S.E. Moradia, et al., J. Alloys Compd. 489 (2010) 168–171.
[5] Y. Saito, Catal. Catal. 47 (2005) 137–139.
[6] F. Sotoodeh, et al., Appl. Catal. A: Gen. 362 (2009) 155–162.
[7] A. Moores, M. Poyatos, Y. Luo, R.H. Crabtree, New J. Chem. 30 (2006) 1675–1678.
[8] D. Vojtech, P. Guhlova, et al., J. Alloys Compd. 494 (2010) 456–462.
[9] R.H. Crabtree, Energy Environ. Sci. 1 (2008) 134–138.
[10] Air Products and Chemicals Project Report, FY2005 Annual Progress Report for the DOE Hydrogen Program, November 2005. Available at: http://www.hydrogen.energy.gov/annual_progress05_storage.html.
[11] G.P. Pez, A.R. Scott, A.C. Cooper, H. Cheng. US Pat, 7,101,530, 2006.
[12] G.P. Pez, A.R. Scott, A.C. Cooper, H. Cheng, F.C. Wilhel, A. Abdourazak. US Pat, 7,351,395, 2008.
[13] K.M. Eblagon, D. Rentsch, O. Friedrichs, et al., Int. J. Hydrogen Energy (2010), doi:10.1016/j.ijhydene.2010.03.068.
[14] Y. An, C.P. Chen, G.H. Xu, et al., J. Rare Earths 20 (2002) 113–115.
[15] Y. An, C.P. Chen, G.H. Xu, et al., J. Rare Earths 20 (2002) 231–233.
[16] E. Alper, Mass Transfer with Chemical Reaction in Multiphase Systems, vol. 2: Three-phase Systems, Martinus Nijhoff, The Hague, 1983.
[17] O. Levenspiel, Chemical Reaction Engineering, John Wiley & Sons, 1972.
[18] R.B. Bird, W.E. Stewart, E.N. Lightfoot, Transport Phenomena, John Wiley & Sons, New York, 1960.